JB Journals.ASM.org

DNA Ligase C1 Mediates the LigD-Independent Nonhomologous End-Joining Pathway of *Mycobacterium smegmatis*

Hitesh Bhattarai,[a] Richa Gupta,[b] Michael S. Glickman[a,b,c]

Weill Cornell Graduate School of Biomedical Sciences, New York, New York, USA[a]; Immunology Program, Sloan Kettering Institute, New York, New York, USA[b]; Division of Infectious Diseases, Memorial Sloan Kettering Cancer Center, New York, New York, USA[c]

Nonhomologous end joining (NHEJ) is a recently described bacterial DNA double-strand break (DSB) repair pathway that has been best characterized for mycobacteria. NHEJ can religate transformed linear plasmids, repair ionizing radiation (IR)-induced DSBs in nonreplicating cells, and seal I-SceI-induced chromosomal DSBs. The core components of the mycobacterial NHEJ machinery are the DNA end binding protein Ku and the polyfunctional DNA ligase LigD. LigD has three autonomous enzymatic modules: ATP-dependent DNA ligase (LIG), DNA/RNA polymerase (POL), and 3′ phosphoesterase (PE). Although genetic ablation of *ku* or *ligD* abolishes NHEJ and sensitizes nonreplicating cells to ionizing radiation, selective ablation of the ligase activity of LigD *in vivo* only mildly impairs NHEJ of linearized plasmids, indicating that an additional DNA ligase can support NHEJ. Additionally, the *in vivo* role of the POL and PE domains in NHEJ is unclear. Here we define a LigD ligase-independent NHEJ pathway in *Mycobacterium smegmatis* that requires the ATP-dependent DNA ligase LigC1 and the POL domain of LigD. *Mycobacterium tuberculosis* LigC can also support this backup NHEJ pathway. We also demonstrate that, although dispensable for efficient plasmid NHEJ, the activities of the POL and PE domains are required for repair of IR-induced DSBs in nonreplicating cells. These findings define the genetic requirements for a LigD-independent NHEJ pathway in mycobacteria and demonstrate that all enzymatic functions of the LigD protein participate in NHEJ *in vivo*.

Chromosomal DNA is under constant attack from clastogens that threaten the coding capacity and stability of the genome. Among the wide variety of DNA lesions that the cell must process, double strand breaks (DSBs) of DNA represent a particularly lethal form of DNA damage that must be repaired for chromosome replication and transcription to proceed. The sources of DSBs include ionizing radiation (IR), replication across a single-stranded nick (1), DNA processing enzymes that generate DSBs, such as topoisomerases, and embedded ribonucleotides in chromosomal DNA (2–5). As such, the repair of DSBs is a critical function in all living organisms, including bacteria. The most intensely studied and universally distributed pathway of DSB repair is RecA-dependent homologous recombination (HR), which uses an intact chromosomal template to repair the DSB without mutation. RecA-dependent HR is the dominant and sole DSB repair pathway in *Escherichia coli*. However, additional pathways of DSB repair operate in other bacteria, including mycobacteria, such as *Mycobacterium smegmatis* and *M. tuberculosis*. *M. smegmatis* elaborates three genetically distinct DNA repair pathways: RecA-dependent HR, single-strand annealing (SSA), and nonhomologous end joining (NHEJ) (6). All mycobacterial HR uses the RecA strand exchange protein, whereas two subpathways utilize the AdnAB helicase-nuclease (6, 7) or RecO (8), respectively. The SSA pathway requires RecBCD (6), which does not participate in HR in mycobacteria, and RecO (8).

Mycobacterial NHEJ can recircularize transformed linear plasmids (9–14), repair IR-induced DSBs in late-stationary-phase cells (15, 16), protect mycobacteria from desiccation (15), and seal homing endonuclease-induced DSBs (6, 16). In all of these experimental systems, the NHEJ pathway requires the DNA end binding protein Ku and the polyfunctional DNA ligase LigD. Genetic ablation of *ku* or *ligD* reduces the efficiency of plasmid NHEJ by approximately 500-fold (10). Similarly, *M. smegmatis* ΔKu or Δ*ligD* bacteria in late stationary phase but not log phase are sensitized to IR (16) and cannot repair I-SceI-induced chromosomal breaks by NHEJ (6). Ablation of *ku* or *ligD* also leads to reciprocal upregulation of the HR pathway in the I-SceI system, suggesting that the NHEJ and HR pathways compete for repair of DSBs in log-phase cells (6).

The LigD protein has three autonomous enzymatic domains: polymerase (POL), phosphoesterase (PE), and ligase (LIG). LigD-POL is a primase-like polymerase that can add both templated and nontemplated deoxynucleoside triphosphates (dNTPs) or ribonucleoside triphosphates (rNTPs) to DNA substrates (13, 17). Alanine substitution mutations at the diaspartate metal binding site of the polymerase (D136A/D138A) abolish polymerase activity *in vitro* (11). *M. smegmatis* expressing LigD-D136/138A cannot add nontemplated nucleotides to blunt end linear plasmid substrates, resulting in a rise in the fidelity of NHEJ with little change in the overall efficiency (10, 13). However, templated fill-in of 5′-overhang NHEJ substrates is not abolished by ablation of POL activity, implicating additional polymerases in these end modifications. The LigD PE domain is a 3′-end-processing enzyme that can resect a tract of ribonucleotides on a primer template, leaving a single ribonucleotide (18, 19). PE also displays phosphodiesterase and monoesterase activities that can process 3′-phosphate-terminated DNA ends to 3′ OH. However, ablation of LigD-PE has no measurable effect on the efficiency or fidelity of plasmid

Received 7 May 2014 Accepted 13 June 2014
Published ahead of print 23 June 2014
Address correspondence to Michael S. Glickman, glickmam@mskcc.org.
Supplemental material for this article may be found at http://dx.doi.org/10.1128/JB.01832-14.
Copyright © 2014, American Society for Microbiology. All Rights Reserved.
doi:10.1128/JB.01832-14

NHEJ (10). Finally, LigD-LIG is an ATP-dependent DNA ligase with a relatively poor nick ligation activity *in vitro* (12). LigD activity is stimulated by the presence of a single ribonucleotide, suggesting that the ribonucleotide addition and processing activities of the POL and PE domains may process the ends to facilitate LigD ligation (20). Interestingly, this ribonucleotide-stimulated nick ligation activity is also exhibited by ligase C (20), an ATP dependent ligase without POL or PE domains whose role *in vivo* is not clear.

Surprisingly, ablation of LigD ligase activity *in vivo* (either through the K484A active site substitution or deletion of the LIG domain) did not reduce plasmid NHEJ substantially (9, 10), in contrast to the severe NHEJ decrement observed with the Δ*ligD* strain. The LigD-independent NHEJ pathway that is evident in the LigD-K484A strain is low fidelity and characterized by frequent deletions at the break site. Deletion of the three additional ATP-dependent DNA ligases in combination (LigB, LigC1, and LigC2) abolishes this backup NHEJ pathway (10), but the responsible ligase has not been further defined.

Using the plasmid-based assay for NHEJ, these prior studies documented the importance of LigD in NHEJ and revealed the existence of a backup NHEJ pathway. However, multiple questions remained unanswered. First, the DSBs in the plasmid assay have "clean" 5′-PO_4/3′-OH ends that do not require end modification for religation. This feature of the plasmid NHEJ assay may obscure the participation of end processing functions of the NHEJ machinery (such as POL and PE), which would be required to repair "dirty" DSBs generated by clastogens that may have 3′ PO_4 and/or require gap filling by a polymerase. Additionally, the molecular participants in the low-fidelity LigD-independent NHEJ pathway, including the DNA ligase, are not known. In this study, we used two assays of chromosomal DSB repair, late-stationary-phase IR sensitivity and I-SceI-induced DSBs, to define the contribution of the LigD-POL and PE domains in repair, define the molecular constituents of the LigD-ligase-independent NHEJ pathway, and examine the expression of NHEJ components in late-stationary-phase mycobacterial cells.

MATERIALS AND METHODS

Strains, plasmids, and oligonucleotides. Bacterial strains are listed in Table S1, plasmids in Table S2, and oligonucleotides in Table S3 in the supplemental material.

NHEJ plasmid assay. The plasmid assay for NHEJ was executed as previously described (10) with blunt-end and 5′-overhang ends. To determine NHEJ efficiency, three replicate transformations were performed, and average values for each were calculated. Kanamycin-resistant transformants that had recircularized the linear plasmid were recovered on agar medium containing kanamycin (20 μg/ml) and 5-bromo-4-chloro-3-indolyl-β-D-galactopyranoside (X-Gal) (50 μg/ml). The numbers of blue and white colonies were enumerated for linear and circular transformations. Efficiency of linear transformation was calculated as the number of transformants per ng of the linear plasmid divided by the number of transformants per ng of the circular plasmid. Efficiency for a given strain was normalized to the efficiency of the wild-type (WT) strain or another reference strain (as appropriate) and expressed as a percentage. Percent fidelity was calculated as number of kanamycin-resistant blue transformants/total number of kanamycin-resistant transformants.

Late-stationary-phase ionizing radiation treatment. The various strains were grown in Difco Middlebrook 7H9 broth supplemented with 0.5% glycerol, 0.5% dextrose, and 0.05% Tween 80 in 200 ml nonbaffled flasks until the optical density at 600 nm (OD_{600}) stabilized in stationary phase. Forty-eight hours later, bacteria were resuspended in phosphate-buffered saline (PBS) with 0.05% Tween 80 and subjected to ionizing radiation (IR) treatment at 600- and 1,200-Gy dosages from a ^{137}Cs source that irradiates at the rate of 10.3 Gy/min in an irradiation chamber equipped with a rotating platform to equalize dosages between samples. Serial dilutions in PBS–0.05% Tween 80 were spotted onto Difco 7H10 plates containing 0.5% glycerol and 0.5% dextrose. Surviving colonies were counted 3 days after incubating at 37°C, and fraction survival was calculated in comparison to unexposed control cells from the same strain. The absolute fractional survival in these assays is somewhat variable between experiments within a 10-fold range, likely due to experimental variability within the radiation chamber and the long exposure times. To control for this variability, we have included relevant control strains in every exposure experiment. An unpaired parametric *t* test was used to compare fraction sensitivity at 1,200 Gy using GraphPad Prism 6.

Chromosomal I-SceI assays. The *M. smegmatis* wild type or the various strains harboring the chromosomally integrated *lacZ* reporter construct (see Table S1 in the supplemental material) were subjected to the plasmid transformation-based I-SceI DSB repair assay as described previously (6). Briefly, equivalent molar amounts of the I-SceI plasmid or control vector plasmid were transformed to determine the frequency of HR, SSA, and NHEJ repair in these strains. For each strain, the experiment was performed at least thrice using different batches of competent cells, and results are expressed as mean values. Since the observed percent survival was similar for all the strains (0.030 [±0.002]), frequencies of different repair outcomes are compared by calculating the relative repair frequency, as follows: relative HR frequency = (HR events/blue events) × (% blue); relative SSA frequency = (SSA events/blue events) × (% blue). Among the blue colonies, the HR and SSA events were distinguished by scoring for kanamycin resistance, whereby the kanamycin-resistant colonies represent HR and kanamycin-sensitive colonies denote SSA. To ascertain mean values for the relative HR and SSA frequencies in different genetic backgrounds, large number of blue colonies (ranging from 60 to 100) were analyzed in separate repeat experiments. To determine NHEJ outcomes in the white colonies, repair junctions were analyzed by PCR amplification and sequencing as described previously (6).

***ligC1*, *ligC2*, *ligB*, and *ligCTB* complementation constructs.** Complementation constructs expressing *M. smegmatis ligC1*, *ligC2*, or *ligB* under their putative native promoters were constructed in the vector pDB60. pDB60 is an *attB*- and L5 integrase-containing vector that integrates into the mycobacterial *attB* site in the chromosome. *M. smegmatis ligC1* and *ligC2* are divergently transcribed in *M. smegmatis* chromosome (see Fig. S1 in the supplemental material). The predicted intergenic region between the LigC1 and LigC2 translation initiation codons is 59 nucleotides (nt) in length. The presumed native promoter of *ligC1* was cloned to contain these 59 nt plus 61 nt from the *ligC2* open reading frame using the primers ligC1_3′ and ligC5′ (see Fig. S1 in the supplemental material). To amplify *ligC2* with its presumed native promoter, 47 nt from the *ligC1* open reading frame were included, in addition to the 59 nt from the intergenic region using the primers ligC3′ and ligC2_5′ (see Fig. S1). *ligB* was cloned with 151 nt upstream of its open reading frame to include its native promoter using the primers LigB_pro_for and LigB_pro_rev. The PCR products containing *ligC1*, *ligC2*, or *ligB* were inserted into the shuttle vector pMSG234 and, after DNA sequencing to exclude mutations, were subcloned into pDB60 to give the plasmids pHB1 (*ligC1*), pHB2 (*ligC2*), and pHB3 (*ligB*). *ligC2* under the constitutive mycobacterial optimized promoter (MOP) was inserted into pDB60 to give the plasmid pHB4. *ligC1* under its native promoter and *ligC2* under its native promoter and the MOP were tagged with a hemagglutinin (HA) tag at the C terminus using the primers "HA tag to LigC2" and "HA into ligC1"and also inserted into pDB60. *ligC* from *M. tuberculosis*, tagged with HA at the C terminus and expressed from the *M. smegmatis ligC1* promoter, was constructed by overlap extension PCR with the primers ligC1_3′, ligCTBwithC1pF, ligCTBwithC1pR, and ligCTBHAtag (see Fig. S1). The PCR product was inserted into pMSG234 and, after DNA sequencing to exclude mutations, inserted into pDB60 to give pHB8. The plasmids pHB1 to -8 were transformed into *ligD*-(K484A) Δ*ligC1-ligC2* Δ*ligB*

(MGM 810) and Δ*ligD* Δ*ligC1-ligC2* Δ*ligB* (MGM 808) strains to yield the strains listed in Table S1.

Immunoblotting. For the determination of the protein levels of LigC isoforms, the appropriate strains were grown to an OD_{600} of 0.4. The cells were collected by centrifugation at 3,700 × *g* and treated with 1 mg/ml lysozyme in TE buffer (10 mM Tris, 1 mM EDTA, pH 8.0) at 37°C for 45 min. The sample was then boiled in SDS-PAGE loading buffer with dithiothreitol (DTT) for 10 min, and proteins were separated by SDS-PAGE in 4 to 12% Bis-Tris acrylamide gels at 200 V for 45 min in morpholinepropanesulfonic acid (MOPS)-SDS running buffer. After transfer to nitrocellulose membrane (Protran; PerkinElmer), HA epitope-tagged proteins were identified by immunoblotting with anti-HA (1:10,000; Covance) and horseradish peroxidase (HRP)-conjugated anti-mouse secondary antibody (1:20,000 dilution; Zymed). Nitrocellulose membranes were stripped with 2% SDS, 6.25 mM Tris-HCl, and 0.8% β-mercaptoethanol at pH 6.8 for 30 min at 37°C and reprobed with anti-CarD monoclonal antibodies and HRP-conjugated anti-mouse secondary antibody as a loading control.

RT-qPCR. To measure mRNA expression, RNA was extracted from bacteria grown to mid-log (0.5 $O.D_{600}$) or late stationary phase (maximum OD_{600} for 12 h) in LB medium containing 0.5% glycerol, 0.5% dextrose, and 0.05% Tween 80. Cells were lysed in TRIzol reagent using Zirconia beads in a Mini-Beadbeater instrument (Biospec). Residual genomic DNA contamination was removed using a Turbo DNA-free kit (Ambion). RNA was additionally purified using the RNeasy minikit (Qiagen). SuperScript III reverse transcriptase (RT; Invitrogen) was used to reverse transcribe the RNA to cDNA using random hexamer primers. Quantitative PCR was carried out with cDNA samples using SYBR green and an Opticon2 real-time fluorescence detector (MJ Research) in biologic triplicates. Amplification of a single product from the quantitative PCR (qPCR) was confirmed by melting-curve analysis. The cycle threshold value (C_T) from qPCR from a given primer set was subtracted from C_T values from primers that amplify the *sigA* gene. The relative level of each mRNA normalized to *sigA* was calculated using the formula $2^{CT - CT(sigA)}$. Control reactions lacking RT were executed with *sigA* primers and yielded C_T values more than 10 cycles higher than those of reactions with RT.

C2FDG β-galactosidase assay. The primers "Ku promoter 5′" and "Ku promoter 3′" were used to amplify the putative *ku* promoter and first 12 nt of the *ku* coding sequence from *M. smegmatis* chromosomal DNA. This PCR product was inserted into pJEM13 (21) to create pMSG335, which contains 721 nt upstream of *ku*, and the coding sequence for the first four amino acids of Ku fused to the *lacZ* reading frame. Wild-type *M. smegmatis* strains transformed with pMSG335 or pJEM13 (promoterless *lacZ*) were collected at an OD_{600} of 0.5, and aliquots were removed, normalized to 10^6 CFU/well by OD_{600} (using a factor of OD_{600} of $1 = 5 \times 10^8$ CFU/ml), and added to a black 96-well plate. 5-Acetylaminofluorescein di-β-D-galactopyranoside (C2FDG) was added to each well to a final concentration of 30 μM. PBS was added to control wells instead of C2FDG to enable calculation of background fluorescence. For each culture, 3 experimental wells and 3 background wells were used. Plates were incubated at 37°C for 3 h, and fluorescence was determined using a Wallace 1420 plate reader with the temperature control set to 37°C and the following filter set: excitation/emission (Ex/Em), 485 ± 20 nm/530 ± 25 nm.

Strain construction. *polD1* was deleted in the *ligD*-(K484A) background as described in reference 14.

RESULTS

Role of the LigD-LIG domain in NHEJ-mediated repair of chromosomal damage. Our prior investigations into the role of each LigD domain in NHEJ efficiency and fidelity used a plasmid recircularization assay in which NHEJ is the only pathway that can repair the plasmid and the ends are compatible due to their generation through restriction endonuclease cleavage. Our prior work has also shown that mycobacterial NHEJ becomes important for IR resistance in late-stationary-phase cells (16), but the role of each LigD structural domain or domain activity in this chromosomal repair phenotype is unknown. To clarify the role of each LigD activity (ligase, phosphoesterase, and polymerase) in chromosomal repair, we measured the stationary-phase IR resistance of strains encoding full-length LigD proteins with inactivating mutations of each LigD domain.

We first investigated the role of the catalytic activity of the LigD-LIG domain in IR resistance by testing *M. smegmatis* wild-type, Δ*ligD*, and *ligD*-(K484A) strains in late stationary phase, the conditions in which NHEJ becomes important for survival. The protein encoded by the *ligD*-(K484A) allele lacks all ligase activity (9, 10, 12). When wild-type *M. smegmatis* was subjected to 600 and 1,200 Gy IR, we observed 0.9- and 2.2-log killing (Fig. 1A and B), whereas the same dosages of IR resulted in 2.2 and 4.8 logs of killing in the Δ*ligD* strain (Fig. 1A and B), confirming our prior findings that LigD is required for DSB repair in late stationary phase (16). The *ligD*-(K484A) strain displays a phenotype intermediate between those of the wild-type and Δ*ligD* strains (Fig. 1A and B), and loss of the entire ligase domain [*ligD*-(ΔLIG)] phenocopied *ligD*-(K484A) (Fig. 1B and C). Specifically, at a dose of 1,200 Gy, the *ligD*-(K484A) and *ligD*-(ΔLIG) strains are 0.7 to 0.9 logs more sensitive than the wild type, whereas the Δ*ligD* strain is about 2.3 logs more sensitive (Fig. 1C). Taken together, these results indicate that loss of the LigD ligase activity, either through active site mutation or domain deletion, does not recapitulate the IR sensitivity observed with loss of the entire LigD protein, implying that an additional ligase can compensate for the loss of LigD ligase activity, provided that the LigD protein is present.

To glean additional insight into the effect of the LIG domain inactivation and deletion on relative frequencies of NHEJ, HR, and SSA, an I-SceI-based assay was employed. This assay can simultaneously assay all three DSB repair pathways in mycobacteria (HR, NHEJ, and SSA), and we have previously shown that loss of NHEJ through genetic ablation of *ku* or *ligD* leads to an upregulation of HR frequency (6). Accordingly, we assayed the frequency of HR in the *ligD*-(K484A) and *ligD*-(ΔLIG) strains. The frequency of HR in the Δ*ligD* strain was 80.9%, a 2-fold increase above that of the WT, as previously reported (6). The *ligD*-(K484A) and *ligD*-(ΔLIG) strains showed 57.8 and 59.0% HR events, respectively, a level intermediate between those of the WT and Δ*ligD* strains (Fig. 1D). To determine the molecular outcomes of NHEJ events in these strains, we amplified the repair junctions from surviving white colonies, which represent a mixture of NHEJ-mediated repair and unmodified sites due to inactivation of the I-SceI enzyme (6). Out of the 42 white colonies of the *ligD*-(K484A) mutant analyzed by PCR amplification and sequencing, 23 showed intact chromosomal loci with unmodified I-SceI sites (~1,350-bp amplification product), whereas 12 events entailed deletions (<2 kb) with the characteristic NHEJ outcomes (bidirectional/unidirectional deletions and cross-break fill-in) that we have previously observed in the wild-type strain (6), indicating that even in the absence of an active LigD ligase domain, the backup NHEJ pathway can function to repair DSBs (see Fig. S2A in the supplemental material). For the remaining 7 repair events, even using primers that anneal farther away from the I-SceI site, PCR products could not be obtained. We surmise that these events reflect large deletions that could not be mapped by the primer pairs used.

Role of LigD-POL domain in NHEJ-mediated repair of chromosomal damage. In our prior plasmid recircularization assays, inactivation of LigD-POL polymerase activity (through

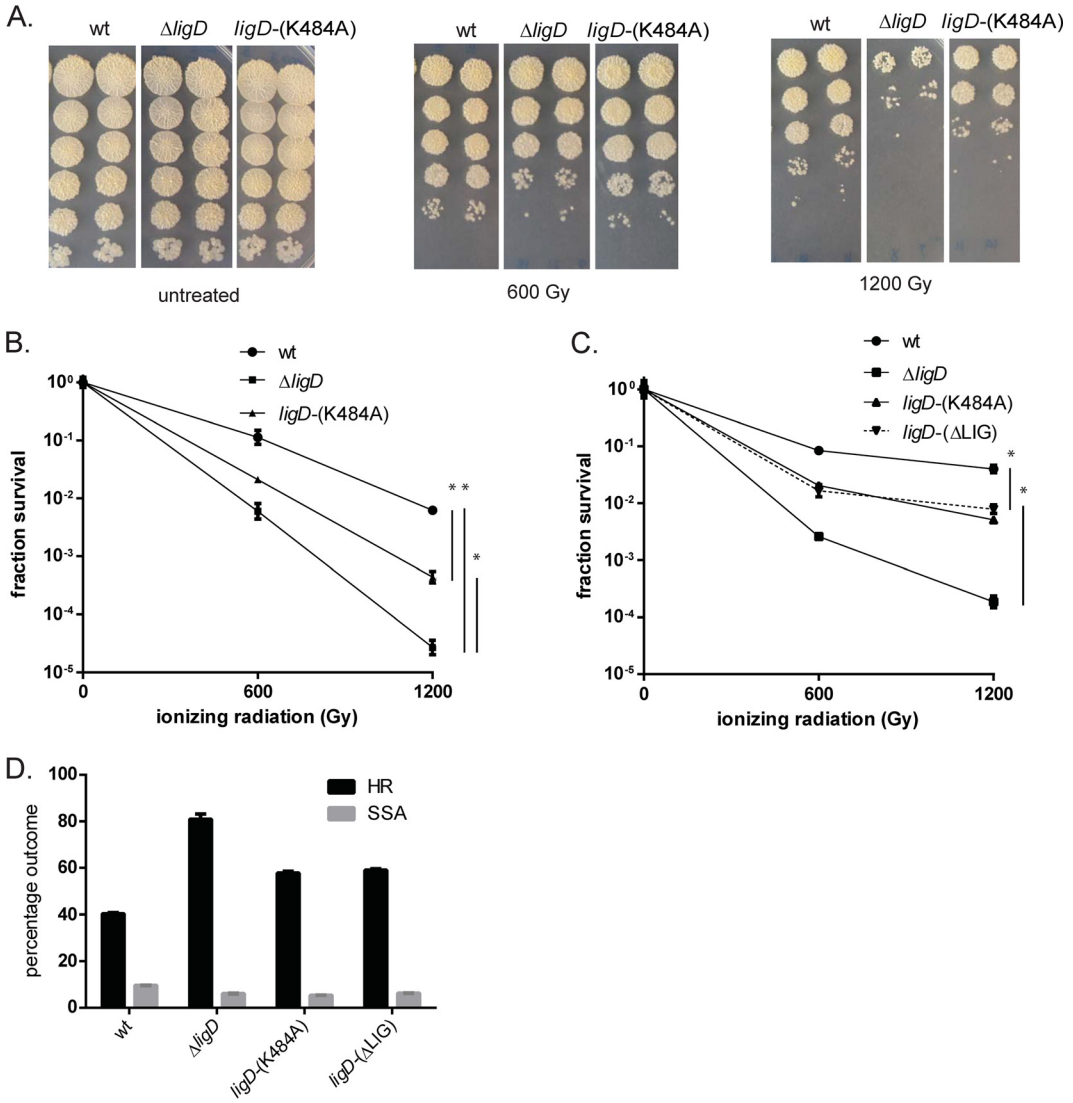

FIG 1 A LigD-LIG-independent NHEJ pathway participates in chromosomal repair. (A) *M. smegmatis ligD*-(K484A) (MGM 803) and *M. smegmatis ligD*-(ΔLIG) (MGM 805) were subjected to 600 and 1,200 Gy of IR after 2 days in late stationary phase in 7H9 minimal medium alongside wild-type and Δ*ligD* (MGM 140) strains. The surviving cells were enumerated as 10-fold serial dilutions. Treatment was carried out on biologic triplicates, and each treatment was spotted in duplicate. (B) Fraction survival of wild-type (wt), *ligD*-(K484A), and Δ*ligD* strains was plotted in log scale with the IR dose on the *x* axis. Statistical significance between strains is indicated by a vertical line, with "*" indicating $P < 0.05$. (C) The fraction survival of wild-type, *ligD*-(ΔLIG), *ligD*-(K484A), and Δ*ligD* strains. (D) The relative frequency of homologous recombination (HR) and single-stranded annealing (SSA) in the chromosomal I-SceI assay for the indicated strains.

the D136A-D138A substitutions) did not affect the efficiency of NHEJ, although the fidelity was raised due to loss of end modifications, particularly at blunt ends, catalyzed by LigD-POL (10, 13, 22). In contrast, deletion of the POL domain from LigD reduced NHEJ to levels of the Δ*ligD* strain, implying a structural role for the POL domain that is independent of its polymerization activity. It is likely that IR-induced DSBs frequently have incompatible ends that must be modified before ligation, potentially requiring the activity of LigD-POL or other polymerases. To test the role of the POL domain in chromosomal DSB repair, we tested the *ligD*-(D136A-D138A) and *ligD*-(ΔPOL) strains for late-stationary-phase IR sensitivity. Surprisingly, *M. smegmatis ligD*-(D136A-D138A) was as sensitive as the Δ*ligD* strain (Fig. 2A and B). Both the *ligD*-(D136A-D138A) and Δ*ligD* strains were 1.3 and 2.4 logs more sensitive than the wild type at 600 and 1,200 Gy, respectively. A similar phenotype was observed for the ΔPOL strain, which was 1.1 and 2.6 logs more sensitive than the wild type at 600 and 1,200 Gy, a sensitization similar to that seen for the Δ*ligD* strain (Fig. 2C). These results implicate the polymerization activity of LigD-POL in repairing IR-induced DSBs and stand in contrast to our prior plasmid assays, in which POL activity was largely dispensable for NHEJ efficiency, likely due to the presence of compatible DSB ends.

To further examine the role of LigD-POL in the repair of chromosomal DNA breaks with incompatible ends, we tested the *ligD*-(D136A-D138A) and *ligD*-(ΔPOL) strains in the I-SceI assay. Both *ligD*-(D136A-D138A) and *ligD*-(ΔPOL) strains demonstrated a mild decrement in relative HR frequency and a mild increase in SSA frequency compared to those of the wild type (Fig. 2D). We next characterized the repair junctions of white colonies

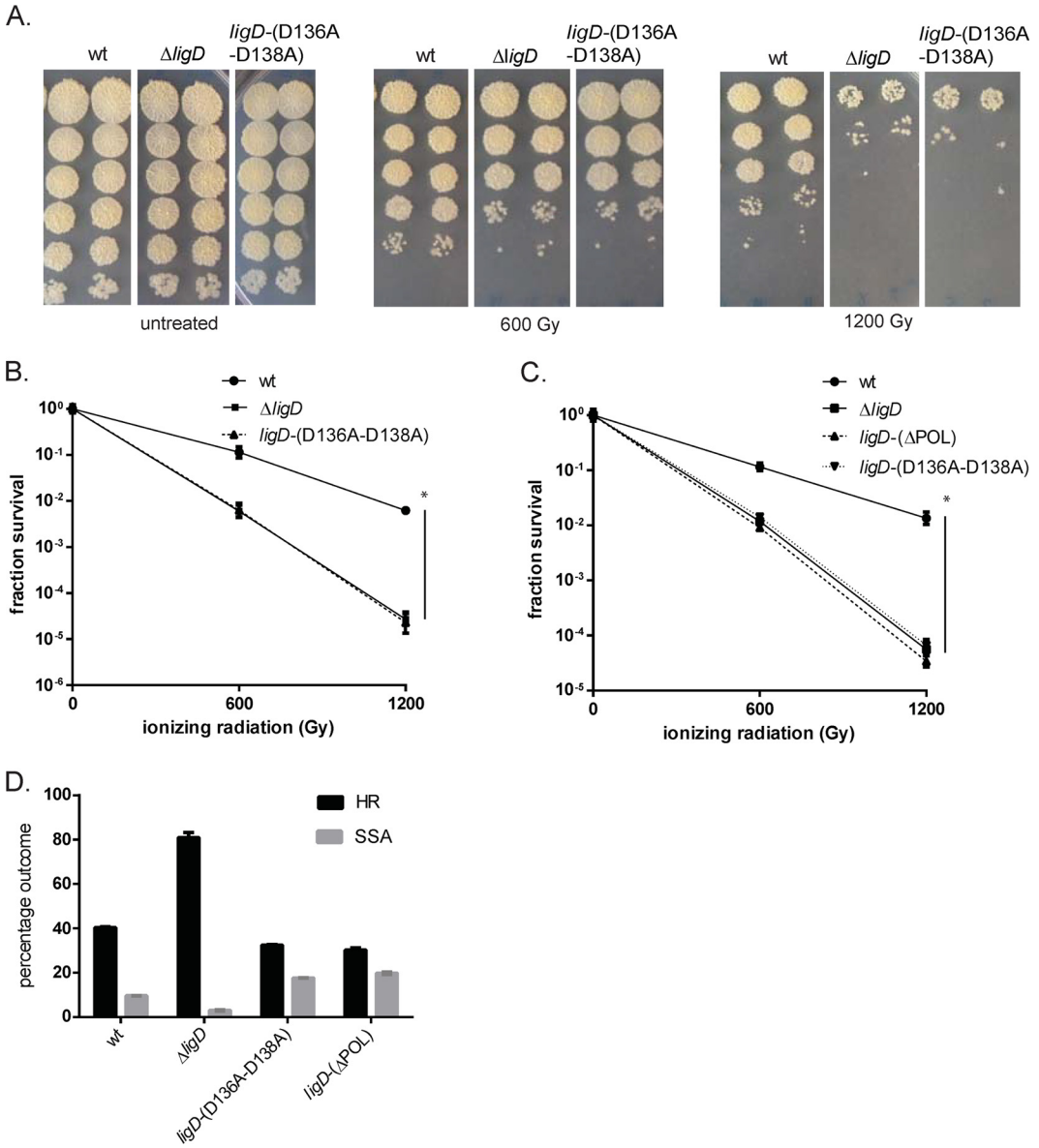

FIG 2 LigD POL activity is required for NHEJ-mediated repair of chromosomal DSBs. (A and B) The wild-type (wt), Δ*ligD* (MGM 140), or *ligD*-(D136A-D138A) (MGM 801) strain was subjected to IR in late stationary phase, duplicate serial 10-fold dilutions were cultured (A), and fraction survival was calculated and plotted in log scale (B). Statistical significance between strains is indicated by a vertical line, with "*" indicating $P < 0.05$. (C) Fraction survival of the *ligD*-(ΔPOL) strain (MGM 802) at 600 and 1,200 Gy IR was plotted alongside that of the wild-type, *ligD*-(D136A-D138A), and Δ*ligD* strains. (D) Relative frequencies of homologous recombination (HR) and single-stranded annealing (SSA) in the chromosomal I-SceI assay for the indicated strains.

surviving I-SceI induction in the *ligD*-(D136A-D138A) strain. Only 1 out of 40 junctions was found to have a short deletion and cross-break priming (see Fig. S2B in the supplemental material). The majority of the junctions (24/40) could not be amplified, suggesting longer deletions, and the remaining 15 events showed intact I-SceI sites, indicating I-SceI inactivation. These results confirm that LigD-POL is required for efficient NHEJ of incompatible I-SceI-generated breaks.

The ability of the LigD-K484A strain but not the Δ*ligD* or ΔPOL strains to support NHEJ implies that the POL domain is necessary for the NHEJ complex to function. To define whether the POL domain is sufficient to support NHEJ-mediated repair of chromosomal breaks independent of the PE and LIG domains, we created a strain that expresses only LigD-POL but lacks both PE and LIG [LigD-(POL only)] and tested its NHEJ proficiency. The *ligD*-(POL only) strain was 0.8 and 1.2 logs more sensitive than the wild type at 600 and 1,200 Gy, a phenotype that recapitulates the *ligD*-(ΔLIG) phenotype (Fig. 3A). We next tested the ability of the POL domain to support NHEJ-mediated plasmid recircularization. NHEJ efficiencies of blunt- and 5′-end linear plasmids were 5.7 and 6.8% of that of the wild type in the *ligD*-(POL only) strain, similar to the efficiency observed for the *ligD*-ΔLIG strain (Fig. 3B). The NHEJ pathway supported by the POL domain was a low-fidelity repair pathway, with fidelity values similar to those

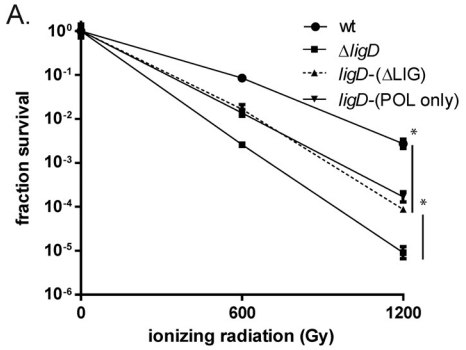

B.

Strain	Efficiency (blunt end)	Fidelity (blunt end)	Efficiency (5′ end)	Fidelity (5′ end)
Wild-type	100	38	100	40
Δ*ligD*	0.13	ND	0.50	ND
ligD-(POL only)	5.7	0.22	6.8	15
ligD-(ΔLIG)	5.3	0.58	5.4	22

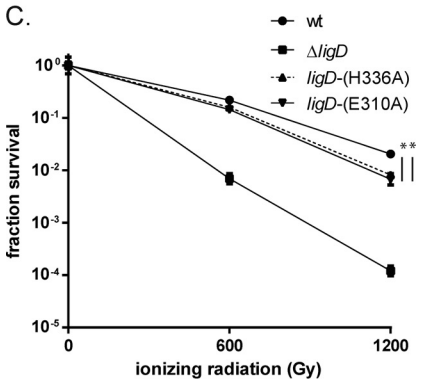

FIG 3 Role of the PE and POL domains in NHEJ. (A) Wild-type (wt), *ligD*-(POL only) (MGM 812), *ligD*-(ΔLIG) (MGM 805), and Δ*ligD* (MGM 140) strains were treated with IR in late stationary phase, and fraction survival for the strains is plotted. Statistical significance between strains is indicated by a vertical line, with "∗" indicating $P < 0.05$. (B) Fidelity and efficiency of plasmid NHEJ for blunt and 5′ ends in the wt, Δ*ligD*, *ligD*-(POL only), and *ligD*-(ΔLIG) strains. (C) Strains carrying inactivating mutations in the PE domain, *ligD*-(E310A) (MGM 806) and *ligD*-(H336A) (MGM 807), were subjected to ionizing radiation at 600 Gy and 1,200 Gy. Fraction survival was plotted alongside that of the wild-type and Δ*ligD* controls.

previously reported for the backup NHEJ pathway that operates independently of LigD ligase activity (9, 10) (Fig. 3B). These data demonstrate that the POL domain is sufficient to support the LigD-LIG-independent NHEJ pathway.

Role of LigD-PE domain in NHEJ-mediated repair of chromosomal damage. Our prior plasmid assays failed to reveal a role for the PE domain in plasmid NHEJ (10). To determine the role of the LigD-PE domain in the repair of chromosomal damage, we studied *M. smegmatis* carrying LigD with inactivating mutations in the LigD-PE domain, LigD-E310A and -H336A. The E310A substitution abolishes only phosphomonoesterase activity, whereas the H336A substitution abolishes both phosphomonoesterase and phosphodiesterase activities (19, 23, 24). Stationary-phase IR experiments indicated that PE inactivation through either mutation conferred a small but statistically significant sensitization to IR of approximately 5-fold at 1,200 Gy (Fig. 3C). These data demonstrate an *in vivo* function for the PE domain in repair of chromosomal DNA damage.

LigC1 is the ligase of the LigD-independent backup NHEJ pathway. Our prior studies have shown that the residual plasmid NHEJ observed in the *ligD*-(K484A) strain is abolished by deletion of the three additional mycobacterial ATP-dependent ligases in combination (encoded by *ligC1*, *ligC2*, and *ligB*) (10). This result indicates that one or more of the three ATP-dependent ligases, LigC1, LigC2, or LigB, can sustain a backup pathway of NHEJ when the LigD ligase domain is inactivated. To further define which ligase supports the backup NHEJ pathway, we complemented *M. smegmatis ligD*-(K484A) Δ*ligC1-ligC2* Δ*ligB* individually with *ligC1*, *ligC2*, or *ligB* under the control of their native promoters and measured NHEJ by plasmid recircularization. As previously reported, NHEJ in the *ligD*-(K484A) strain is efficient but low fidelity. NHEJ efficiency is 38 and 59% for blunt-end and 5′-end NHEJ, respectively, compared to that of the wild type (Table 1). The fidelity was 0.25% for blunt-end ligation and 5.5% for 5′-end ligation. NHEJ efficiency dropped to 0.08 and 0.13 when

TABLE 1 Plasmid assay with 5′ overhang and blunt ends for the wild-type strain and variants[a]

Genotype	NHEJ analysis[b]			
	Blunt end		5′ overhang end	
	% efficiency	% fidelity	% efficiency	% fidelity
Wild type	100	52	100	28
ligD-(K484A)	38	0.25	59	5.5
ligD-(K484A) Δ*ligB-ligC*	0.08	ND	0.13	ND
ligD-(K484A) Δ*ligB-ligC attB*::*ligC1*	23.3	0.31	22	4.2
ligD-(K484A) Δ*ligB-ligC attB*::*ligC2*	0.04	ND	0.03	ND
ligD-(K484A) Δ*ligB-ligC attB*::*ligB*	0.08	ND	0.06	ND

[a] Wild-type, *ligD*-(K484A) (MGM 835h), *ligD*-(K484A) Δ*ligC1-ligC2* Δ*ligB* (MGM 832h), *ligD*-(K484A) Δ*ligC1-ligC2* Δ*ligB attB*::*nat_ligC1* (MGM 839h), *ligD*-(K484A) Δ*ligC1-ligC2* Δ*ligB attB*::*nat_ligC2* (MGM 840h), and *ligD*-(K484A) Δ*ligC1-ligC2* Δ*ligB attB*::*nat_ligB* (MGM 833h) strains were analyzed.

[b] Efficiency and fidelity of recircularization of linear plasmids with 5′ overhang ends and blunt ends were calculated as described in Materials and Methods. ND, not determined.

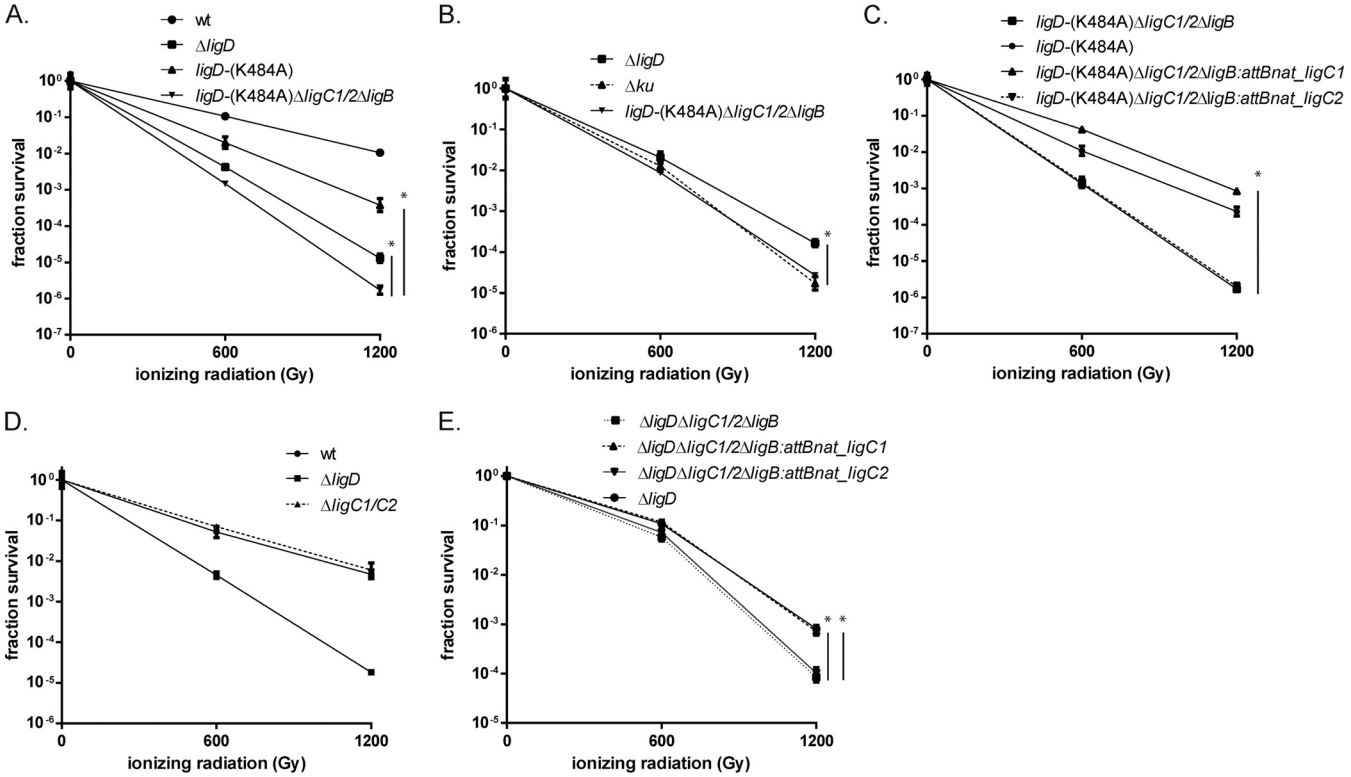

FIG 4 LigC1 is the ligase of the LigD-independent NHEJ pathway. Late-stationary-phase IR sensitivity of the wild-type, Δ*ligD* (MGM 140), *ligD*-(K484A) Δ*ligC1-ligC2* Δ*ligB* (MGM 810), and *ligD*-(K484A) (MGM 803) strains (A), Δ*ku* (MGM 154), Δ*ligD*, and *ligD*-(K484A) Δ*ligC1-ligC2* Δ*ligB* strains (B), *ligD*-(K484A) (MGM 835h) and *ligD*-(K484A) Δ*ligC1-ligC2* Δ*ligB* (MGM 832h) strains, the *ligD*-(K484A) Δ*ligC1-ligC2* Δ*ligB* strain complemented with *ligC1* (MGM 839h), or the *ligC2* (MGM 840h) strain (C), wild-type, Δ*ligD*, and Δ*ligC1-ligC2* (MGM 139) strains (D), or the Δ*ligD* (MGM 858h) or Δ*ligD* Δ*ligC* Δ*ligB* (MGM 859h) strain, the Δ*ligD* Δ*ligC* Δ*ligB* strain complemented with *ligC1* (MGM 860h), or the *ligC2* (MGM 861h) strain (E) is shown. Statistical significance between strains is indicated by a vertical line, with "∗" indicating $P < 0.05$.

ligC1, *ligC2*, and *ligB* were deleted in the *ligD*-(K484A) strain, as previously reported (Table 1). Complementation by *ligC1* restored NHEJ efficiency to the level of the *ligD*-(K484A) strain, indicating that LigC1 provides the backup ligation activity when LigD-LIG is inactivated (Table 1). This LigC1-mediated NHEJ pathway also was low fidelity, with fidelity of 0.31% (blunt ends) or 4.2% (5′ end), similar to that observed in the *ligD*-(K484A) strain. In contrast, complementation with *ligC2* or *ligB* had no measurable effect on the efficiency of NHEJ in the *ligD*-(K484A) Δ*ligC1-ligC2* Δ*ligB* strain (Table 1).

To determine whether the molecular outcomes in the *ligD*-(K484A) Δ*ligC1-ligC2* Δ*ligB attB*::*nat_ligC1* strain (where *nat_ligC1* indicates the native promoter for *ligC1*) are similar to those observed in the *ligD*-(K484A) strain, we determined the nucleotide sequences of religated plasmids from unfaithful (white) NHEJ events in these two strains. Eight out of nine junctions in the *ligD*-(K484A) strain and 10 out of 12 junctions in the *ligD*-(K484A) Δ*ligC1-ligC2* Δ*ligB attB*::*nat_ligC1* strain showed deletions at the blunt end (see Fig. S3 in the supplemental material). Only two events from each strain had nontemplated additions (see Fig. S3). Sequence analysis of 5′-end junctions revealed that all the unfaithful NHEJ events from the *ligD*-(K484A) and *ligD*-(K484A) Δ*ligC1-ligC2* Δ*ligB attB*::*nat_ligC1* strains comprised deletions at the junction (see Fig. S4). Only 2 out of 8 repair events in the *ligD*-(K484A) strain show templated addition, whereas 6 out of 9 *ligD*-(K484A) Δ*ligC1-ligC2* Δ*ligB attB*::*nat_ligC1* clones show templated additions (see Fig. S4). These results demonstrate that LigC1 is the only ATP-dependent ligase capable of compensating for the loss of LigD ligase activity and that the LigC1-mediated backup NHEJ pathway is competent for plasmid NHEJ, albeit at low fidelity.

LigC1 can substitute for LigD-LIG in chromosomal repair. To assess the role of the LigC1-mediated NHEJ pathway in the repair of chromosomal damage, the *ligD*-(K484A) Δ*ligC1-ligC2* Δ*ligB* strain was subjected to IR in late stationary phase along with the wild-type, Δ*ligD*, and *ligD*-(K484A) strains. The *ligD*-(K484A) Δ*ligC1-ligC2* Δ*ligB* strain was not only more sensitive than the *ligD*-(K484A) strain but was also more sensitive than the Δ*ligD* strain (Fig. 4A). The late-stationary-phase IR sensitivity of the *ligD*-(K484A) Δ*ligC1-ligC2* Δ*ligB* strain was similar to that of the Δ*Ku* strain (Fig. 4B). To test whether *ligC1* or *ligC2* is sufficient to support chromosomal repair, we tested the *ligD*-(K484A) Δ*ligC1-ligC2* Δ*ligB* strain with either *ligC1* or *ligC2* and observed that *ligC1*, but not *ligC2*, restored IR resistance to the level of that of the *ligD*-(K484A) strain (Fig. 4C). To test whether *ligC1* or *ligC2* contributes to chromosomal repair in a cell with wild-type LigD, we tested the Δ*ligC1-ligC2* strain and observed no sensitization (Fig. 4D), confirming that LigC functions only in a backup role when LigD ligase is nonfunctional.

The experiments above indicate that LigC1 can compensate for the loss of the LigD ligase when the LigD protein is still present. To test whether *ligC1* or *ligC2* has a function in repair when LigD is

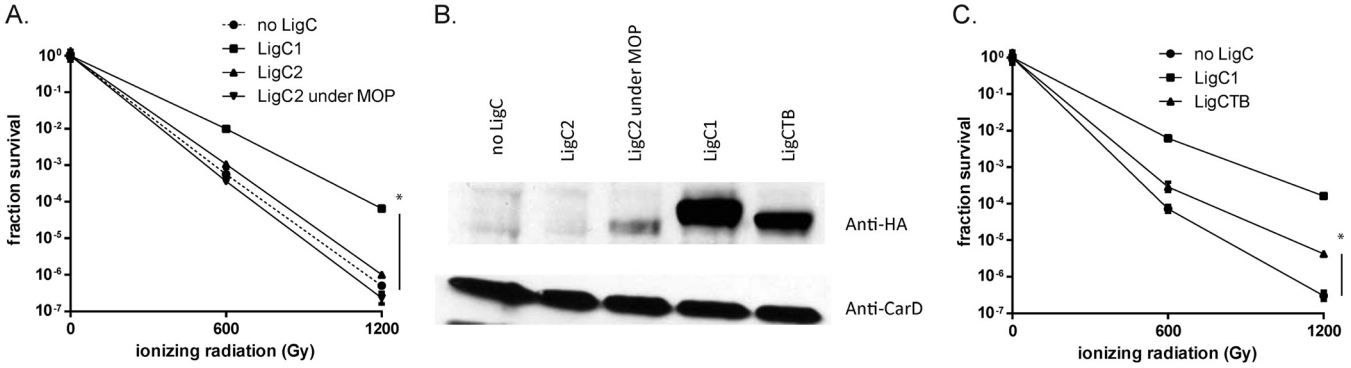

D.

Isoform of LigC	Efficiency (blunt end)	Fidelity (blunt end)	Efficiency (5′ end)	Fidelity (5′ end)
LigC1	100	0.88	100	5.9
LigC2 under MOP	0.24	ND	0.52	ND
LigCTB	56	0.28	47	3.3
no LigC	0.36	ND	0.56	ND

FIG 5 *M. tuberculosis* LigC can support LigD-independent NHEJ. (A and C) Late-stationary-phase IR sensitivities of the *ligD*-(K484A) Δ*ligC1-ligC2* Δ*ligB* strain complemented with vector (no LigC) (MGM 832h), *M. smegmatis* LigC1-HA (MGM 865h), *M. smegmatis* LigC2-HA (MGM 863h), *M. smegmatis* MOP-LigC2-HA (MGM 864h), or *M. tuberculosis* LigC-HA (MGM 866h) strains. Statistical significance between strains is indicated by a vertical line, with "*" indicating $P < 0.05$. (B) Relative expression of the indicated HA-tagged LigC proteins was assessed using anti-HA antibodies and anti-CarD antibody as loading control. (D) Plasmid assay of backup NHEJ in the same strains used in panels A to C, with LigC1 set to 100%.

completely absent, we tested the Δ*ligD* Δ*ligC1-ligC2* Δ*ligB*, Δ*ligD* Δ*ligC1-ligC2* Δ*ligB attB*::*nat_ligC1*, Δ*ligD* Δ*ligC* Δ*ligB*::*nat_ligC2*, and Δ*ligD* strains. The Δ*ligD* Δ*ligC1-ligC2* Δ*ligB* strain was 0.3 and 1.0 logs more sensitive than the Δ*ligD* strain at 600- and 1,200-Gy dosages of IR, indicating a role for *ligB* or *ligC* in late-stationary-phase IR resistance in the absence of LigD. Complementation with *ligC1* restored sensitivity of the Δ*ligD* Δ*ligC1-ligC2* Δ*ligB* strain to Δ*ligD* strain levels, but complementation with *ligC2* did not, indicating that LigC1 mediates clastogen resistance when LigD is absent (Fig. 4E). Taken together, these results indicate that LigC1 functions in chromosomal repair and can function in cells lacking the entire LigD protein.

The differential ability of *ligC1* and *ligC2* to support NHEJ is surprising insofar as the LigC1 and LigC2 proteins are highly homologous. There is 49% amino acid sequence identity between LigC1 and LigC2 (see Fig. S5 in the supplemental material). There is only one LigC protein in *M. tuberculosis*, encoded by the *rv3731* gene. *M. tuberculosis* LigC is more homologous to LigC2 and shows 73% sequence identity to LigC2 versus 49% identity to LigC1 (see Fig. S5). To investigate whether the failure of LigC2 to support NHEJ is due to differences in expression, we generated *ligC1* and *ligC2* complementing alleles encoding hemagglutinin epitope-tagged proteins at their C termini. We also placed the expression of *ligC2* under control of the strong constitutive MOP. LigC1-HA complemented the IR sensitivity phenotype of the *ligD*-(K484A) Δ*ligC1-ligC2* Δ*ligB* strain, but neither native LigC2-HA nor MOP-LigC2-HA was able to restore IR resistance (Fig. 5A). We compared the levels of LigC1-HA and LigC2-HA by immunoblotting and found no detectable LigC2 when expressed from its native promoter, whereas LigC1-HA was easily detectable (Fig. 5B). MOP-LigC2 was detectable but at a lower level than the LigC1 protein (Fig. 5B, lane 3).

LigC from *M. tuberculosis* can substitute for LigD in NHEJ repair. *M. tuberculosis* has only one LigC protein, which is more similar to *M. smegmatis* LigC2 than LigC1 (see Fig. S5 in the supplemental material), possibly suggesting that *M. tuberculosis* LigC does not substitute for LigC1 in the NHEJ pathway. To test this idea, we complemented the *ligD*-(K484A) Δ*ligC1-ligC2* Δ*ligB* strain with *M. tuberculosis* LigC-HA expressed from the *M. smegmatis* LigC1 promoter. LigCTB expressed from the *ligC1* promoter was able to partially restore resistance to IR in late stationary phase (Fig. 5C), although not to the level achieved by LigC1 complementation (Fig. 5C). We next tested whether LigC from *M. tuberculosis* could support the backup pathway of plasmid NHEJ. LigC2-HA expressed under a MOP did not support plasmid NHEJ via the backup pathway (Fig. 5D). However, LigCTB-HA expressed from the *ligC1* promoter was able to restore NHEJ almost to the level of that supported by LigC1 (56% and 47% blunt-end and 5′-end ligation efficiencies [Fig. 5D]). The blunt-end and 5′-end fidelity values were 0.28 and 3.3%, compared to 0.88 and 5.9% for the LigC1-HA-complemented strain (Fig. 5D). LigCTB-HA was expressed at levels higher than LigC2 under a MOP but not as well as LigC1-HA (Fig. 5B, lane 5). RT-qPCR experiments confirmed that all three LigC genes (*ligC1*, *ligC2*, and *M. tuberculosis ligC*) are expressed, indicating that the lack of the LigC2 protein is due to posttranscriptional or posttranslational regulation (see Fig. S6A, B, and C in the supplemental material). These results demonstrate that *M. tuberculosis* LigC is capable of supporting the mycobacterial LigD-independent NHEJ pathway. We cannot determine with certainty whether the noncomplementation by LigC2 is due to poor expression or is an intrinsic property of the LigC2 ligase, but the similarity of *M. tuberculosis* LigC to LigC2 and the higher expression of *M. tuberculosis* LigC suggest that the low expression level of the LigC2 protein may be responsible for its inactivity *in vivo*.

A role for PolD1 and PolD2 in chromosomal repair. LigC1 is encoded in an apparent operon with *polD1*, encoding a freestanding LigD-POL-like polymerase. We have previously characterized

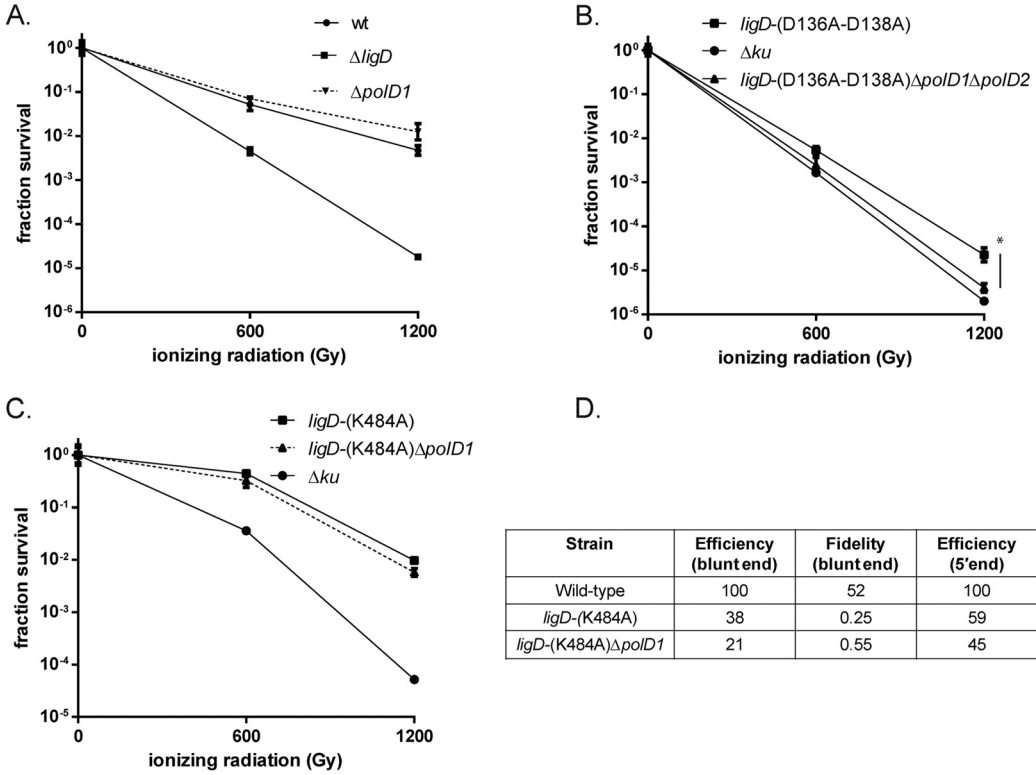

Strain	Efficiency (blunt end)	Fidelity (blunt end)	Efficiency (5′end)	Fidelity (5′end)
Wild-type	100	52	100	28
ligD-(K484A)	38	0.25	59	5.5
ligD-(K484A)Δ*polD1*	21	0.55	45	2.7

FIG 6 Role of PolD1 and PolD2 in NHEJ. Late-stationary-phase IR sensitivity of wild-type, Δ*ligD*, and Δ*polD1* (MGM 843) strains. (B to D) *ligD*-(D136A-D138A) (MGM 801), *ligD*-(D136A-D138A) Δ*polD1* Δ*polD2* (MGM 846), and Δ*ku* (MGM 154) strains (B), *ligD*-(K484A) (MGM 803), *ligD*-(K484A) Δ*polD1* (MGM 844h), and Δ*ku* (MGM 154) strains (C), or plasmid NHEJ assay with 5′-overhang and blunt-end plasmids (D). Statistical significance between strains is indicated, with "*" indicating $P < 0.05$.

the PolD1 and PolD2 proteins and demonstrated that their biochemical activities are similar to those of LigD-POL (14), but deletion of PolD1 and PolD2 in combination did not affect plasmid NHEJ (14). However, given our findings that *M. smegmatis ligD*-(D136A-D138A) is highly sensitized to IR, we readdressed the possibility that PolD1 and PolD2 participate in NHEJ-mediated repair of chromosomal breaks. The Δ*polD1* strain showed no more IR sensitivity than the wild type (Fig. 6A). We next tested the *ligD*-(D136A-D138A) Δ*polD1* Δ*polD2* strain alongside the *ligD*-(D136A-D138A) and Δ*ku* strains and observed that the *ligD*-(D136A-D138A) Δ*polD1* Δ*polD2* strain was 0.3 and 0.8 logs more sensitive than the *ligD*-(D136A-D138A) strain at 600 and 1,200 Gy ($P < 0.05$) and phenocopied the Δ*ku* strain (Fig. 6B). PolD1 did not contribute to NHEJ in the LigD-K484A strain, in which the backup NHEJ pathway is supporting NHEJ (Fig. 6C and D).

Relative levels of *ku*, *ligD*, *ligC1*, and *ligC2* mRNA in mid-log and late stationary phases. Since NHEJ is required for DSB repair in late stationary phase, we hypothesized that the critical mediators of the NHEJ pathway may be upregulated during this growth phase. We used RT-qPCR to measure the mRNA levels of *ku*, *ligD*, *ligC1*, and *ligC2* (all normalized to *sigA*) in mid-log- and late-stationary-phase *M. smegmatis*. The mRNA encoding Ku was upregulated 8-fold in stationary phase compared to levels in log phase, whereas *ligC1* was unchanged and *ligD* and *ligC2* were upregulated 2-fold (see Fig. S7A to D in the supplemental material). We confirmed the upregulation of the *ku* promoter using a *ku* promoter-*lacZ* fusion. *ku* promoter activity was substantially upregulated when the cells were left in late stationary phase for more than 12 h (see Fig. S7E).

DISCUSSION

A LigD-independent pathway of NHEJ in mycobacteria. Our studies further define an NHEJ mechanism in *M. smegmatis* that operates independently of the LigD ligase. Our prior studies indicated that the efficient NHEJ observed in the absence of LigD ligase was mediated by one of the three additional ATP-dependent DNA ligases in the *M. smegmatis* proteome. In this work, we identified LigC1 as the additional NHEJ ligase. Importantly, the LigC1 pathway also requires the LigD-POL domain, which can support NHEJ as an isolated domain independent of LIG or PE, and Ku. The model that emerges from these data is that Ku, LigD-POL, and LigC1 are capable of forming a functional NHEJ complex. Ku interacts directly with LigD-POL (25), and this interaction has been hypothesized to recruit LigD to the broken ends. Structural data also implicate LigD-POL as a synaptic factor that can bridge broken DNA ends, further supporting its central role in nucleating the NHEJ complex (26). Our data would suggest that LigC1 can interact directly with Ku or LigD-POL, although our attempts to identify LigC interactors have not identified either of these two proteins (H. Bhattarai and M. S. Glickman, unpublished data).

Substantial biochemical data complement our genetic findings implicating LigC in NHEJ. In contrast to LigD proteins, LigC proteins are minimized DNA ligases without the additional domains present in LigD. *M. smegmatis* LigC1 is a poor nick-sealing enzyme *in vitro* (12). However, the ligation activity of LigC from *Agrobacterium* is stimulated by Ku, as is that of LigD (27), suggesting that LigC and Ku form a physical complex which is functionally important. *Agrobacterium* LigC and LigD are both stimulated

by the presence of a single ribonucleotide at the break, strongly suggesting that the ribonucleotides added by LigD-POL and trimmed by PE stimulate ligation (20). However, as mentioned above, the LigC protein does not contain POL or PE domains, and therefore its stimulation by a ribonucleotide rationalizes the functional interaction with LigD-POL documented here.

Requirement for PE and POL in chromosomal repair. Our data also identify important functions for the LigD polymerase and PE domains in chromosomal repair. Our prior efforts to document a function for these LigD enzymatic modules in NHEJ had not revealed a role for the PE domain. This lack of phenotype was likely due to the irrelevance of a 3′-end processing activity for a restriction endonuclease-generated 5′ overhang or blunt end. The PE domain acts on 3′-phosphate-terminated ends to regenerate a 3′ hydroxyl which can be ligated by ligase or further extended by polymerase. This activity is stimulated by a 5′ single-stranded tail, suggesting that PE acts at recessed 3′ ends (18). PE activity is thus likely to be important during NHEJ-mediated repair of clastogen-induced DSBs that may generate 3′ phosphate but would be irrelevant for restriction endonuclease-generated ends, which contain 5′ phosphates. Inactivation of the PE domain impaired the survival of *M. smegmatis* under late-stationary-phase IR exposure, although the degree of sensitization was less dramatic (5-fold) than loss of LigD or the POL domain (see below). The mild phenotype of PE inactivation is logical insofar as only a minority of IR-induced breaks will have recessed 3′ phosphates. Approximately half of the 3′ termini generated by IR treatment of DNA *in vitro* have 3′ phosphates (28), confirming that only a subset of the IR-induced breaks would require PE for processing.

The data presented here also strongly revise our view of the importance of the POL domain in NHEJ. In prior experiments, inactivation of the POL domain did change the fidelity of plasmid NHEJ but had minimal effects on NHEJ efficiency. In contrast, LigD-POL activity is absolutely required for IR resistance in late stationary phase, such that the *ligD*-(D136A-D138A) strain is as sensitive as the Δ*ligD* strain. This observation suggests that all LigD-mediated repair of IR-induced chromosomal damage requires polymerization by LigD-POL, which is consistent with the complexity of the damage induced by this clastogen. Our experiments also indicate a role for the PolD enzymes in IR resistance when LigD-POL is inactivated, confirming that these enzymes participate in DSB repair. The LigD-POL-like enzymes PolD1 and PolD2, are biochemically similar to LigD-POL (14) in their ability to add templated and nontemplated nucleotides and their preference for ribonucleotides over dNTPs. Our experiments indicate substantial redundancy between LigD-POL and PolD1/PolD2, such that the combined loss of PolD1/PolD2 impairs NHEJ only when LigD-POL is inactive. The central role of LigD-POL in NHEJ-mediated repair of IR-induced chromosomal damage also suggests that ribonucleotide incorporation into the chromosome is a frequent event during NHEJ-mediated repair. Ribonucleotides are more abundant than dNTPs even in log-phase cells, and recent literature indicates that replicative polymerases frequently incorporate rNTPs into chromosomal DNA, the removal of which by RNase H2 is required to maintain genomic integrity (3, 4, 29–31). Our data suggest that such rNTP incorporation may also be a frequent event during mycobacterial NHEJ and suggest that a system to remove embedded ribonucleotides may cooperate with the NHEJ system.

Comparison to ligase IV-independent NHEJ in eukaryotes. Our finding that an alternative DNA ligase, LigC, can substitute for LigD is conceptually reminiscent of the situation in yeast and mammalian NHEJ. The primary NHEJ ligase in eukaryotic cells is DNA ligase IV (32–34). However, cells lacking LigIV can still execute end joining, including class switch recombination in B cells (35–37). Similarly, yeast carrying an inactivating lysine mutation in LigIV exhibits a backup NHEJ pathway which may be mediated by DNA ligase 1 (38). This LigIV-independent pathway, variously termed alt-NHEJ, nc-NHEJ, or backup NHEJ (b-NHEJ) (1), is characterized by large deletions and frequent use of microhomology at the junctions. The DNA ligase that supports the alternative NHEJ pathway of mammalian cells is not completely clear but likely is a combination of DNA ligase III and DNA ligase I (39–41). The LigD-independent NHEJ pathway examined here is similar in its use of an alternative DNA ligase and its low fidelity with frequent deletions. However, LigD-independent NHEJ in mycobacteria is dependent on Ku and also requires the POL domain of LigD and is therefore apparently distinct, in both its genetic requirements and overall efficiency of repair, from the Ku- and LigD-independent NHEJ of plasmid substrates we have previously described (10). It remains unclear, both in the mycobacterial system demonstrated here and in eukaryotic NHEJ systems, whether the ability of alternative DNA ligases to support NHEJ in the absence of the primary NHEJ ligase represents a true alternative "pathway" that operates in wild-type cells or a "substitution" of a ligation activity supplied by an alternative ligase (42). Regardless of the nomenclature chosen, our results indicate that LigC1 can substantially replace LigD ligase in cells that retain both the LigD-POL domain and Ku.

In summary, we have further elucidated the genetic requirements for NHEJ in mycobacteria. We find that all enzymatic activities of the LigD protein are required for NHEJ. We also find that there is a fully competent NHEJ mechanism that is active in cells lacking LigD-LIG and that this pathway requires LigC1, Ku, and the POL domain of LigD.

ACKNOWLEDGMENTS

This work was supported by NIH grant AI64693 (to M.S.G.) and P30 CA 008748.

REFERENCES

1. **Lieber MR.** 2010. The mechanism of double-strand DNA break repair by the nonhomologous DNA end-joining pathway. Annu. Rev. Biochem. **79:**181–211. http://dx.doi.org/10.1146/annurev.biochem.052308.093131.
2. **Nick McElhinny SA, Kumar D, Clark AB, Watt DL, Watts BE, Lundstrom EB, Johansson E, Chabes A, Kunkel TA.** 2010. Genome instability due to ribonucleotide incorporation into DNA. Nat. Chem. Biol. **6:**774–781. http://dx.doi.org/10.1038/nchembio.424.
3. **Williams JS, Smith DJ, Marjavaara L, Lujan SA, Chabes A, Kunkel TA.** 2013. Topoisomerase 1-mediated removal of ribonucleotides from nascent leading-strand DNA. Mol. Cell **49:**1010–1015. http://dx.doi.org/10.1016/j.molcel.2012.12.021.
4. **Lazzaro F, Novarina D, Amara F, Watt DL, Stone JE, Costanzo V, Burgers PM, Kunkel TA, Plevani P, Muzi-Falconi M.** 2012. RNase H and postreplication repair protect cells from ribonucleotides incorporated in DNA. Mol. Cell **45:**99–110. http://dx.doi.org/10.1016/j.molcel.2011.12.019.
5. **Reijns MA, Rabe B, Rigby RE, Mill P, Astell KR, Lettice LA, Boyle S, Leitch A, Keighren M, Kilanowski F, Devenney PS, Sexton D, Grimes G, Holt IJ, Hill RE, Taylor MS, Lawson KA, Dorin JR, Jackson AP.** 2012. Enzymatic removal of ribonucleotides from DNA is essential for mammalian genome integrity and development. Cell **149:**1008–1022. http://dx.doi.org/10.1016/j.cell.2012.04.011.
6. **Gupta R, Barkan D, Redelman-Sidi G, Shuman S, Glickman MS.** 2011. Mycobacteria exploit three genetically distinct DNA double-strand break repair pathways. Mol. Microbiol. **79:**316–330. http://dx.doi.org/10.1111/j.1365-2958.2010.07463.x.

7. **Sinha KM, Unciuleac M-CC, Glickman MS, Shuman S.** 2009. AdnAB: a new DSB-resecting motor-nuclease from mycobacteria. Genes Dev. **23:** 1423–1437. http://dx.doi.org/10.1101/gad.1805709.
8. **Gupta R, Ryzhikov M, Koroleva O, Unciuleac M, Shuman S, Korolev S, Glickman MS.** 2013. A dual role for mycobacterial RecO in RecA-dependent homologous recombination and RecA-independent single-strand annealing. Nucleic Acids Res. **41:**2284–2295. http://dx.doi.org/10.1093/nar/gks1298.
9. **Akey D, Martins A, Aniukwu J, Glickman MS, Shuman S, Berger JM.** 2006. Crystal structure and nonhomologous end-joining function of the ligase component of Mycobacterium DNA ligase D. J. Biol. Chem. **281:** 13412–13423. http://dx.doi.org/10.1074/jbc.M513550200.
10. **Aniukwu J, Glickman MS, Shuman S.** 2008. The pathways and outcomes of mycobacterial NHEJ depend on the structure of the broken DNA ends. Genes Dev. **22:**512–527. http://dx.doi.org/10.1101/gad.1631908.
11. **Gong C, Bongiorno P, Martins A, Stephanou NC, Zhu H, Shuman S, Glickman MS.** 2005. Mechanism of nonhomologous end-joining in mycobacteria: a low-fidelity repair system driven by Ku, ligase D and ligase C. Nat. Struct. Mol. Biol. **12:**304–312. http://dx.doi.org/10.1038/nsmb915.
12. **Gong C, Martins A, Bongiorno P, Glickman M, Shuman S.** 2004. Biochemical and genetic analysis of the four DNA ligases of mycobacteria. J. Biol. Chem. **279:**20594–20606. http://dx.doi.org/10.1074/jbc.M401841200.
13. **Zhu H, Nandakumar J, Aniukwu J, Wang LK, Glickman MS, Lima CD, Shuman S.** 2006. Atomic structure and nonhomologous end-joining function of the polymerase component of bacterial DNA ligase D. Proc. Natl. Acad. Sci. U. S. A. **103:**1711–1716. http://dx.doi.org/10.1073/pnas.0509083103.
14. **Zhu H, Bhattarai H, Yan HG, Shuman S, Glickman MS.** 2012. Characterization of Mycobacterium smegmatis PolD2 and PolD1 as RNA/DNA polymerases homologous to the POL domain of bacterial DNA ligase D. Biochemistry **51:**10147–10158. http://dx.doi.org/10.1021/bi301202e.
15. **Pitcher RS, Green AJ, Brzostek A, Korycka-Machala M, Dziadek J, Doherty AJ.** 2007. NHEJ protects mycobacteria in stationary phase against the harmful effects of desiccation. DNA Repair **6:**1271–1276. http://dx.doi.org/10.1016/j.dnarep.2007.02.009.
16. **Stephanou NC, Gao F, Bongiorno P, Ehrt S, Schnappinger D, Shuman S, Glickman MS.** 2007. Mycobacterial nonhomologous end joining mediates mutagenic repair of chromosomal double-strand DNA breaks. J. Bacteriol. **189:**5237–5246. http://dx.doi.org/10.1128/JB.00332-07.
17. **Wright D, DeBeaux A, Shi R, Doherty AJ, Harrison L.** 2010. Characterization of the roles of the catalytic domains of Mycobacterium tuberculosis ligase D in Ku-dependent error-prone DNA end joining. Mutagenesis **25:**473–481. http://dx.doi.org/10.1093/mutage/geq029.
18. **Zhu H, Shuman S.** 2006. Substrate specificity and structure-function analysis of the 3′-phosphoesterase component of the bacterial NHEJ protein, DNA ligase D. J. Biol. Chem. **281:**13873–13881. http://dx.doi.org/10.1074/jbc.M600055200.
19. **Zhu H, Shuman S.** 2005. Novel 3′-ribonuclease and 3′-phosphatase activities of the bacterial non-homologous end-joining protein, DNA ligase D. J. Biol. Chem. **280:**25973–25981. http://dx.doi.org/10.1074/jbc.M504002200.
20. **Zhu H, Shuman S.** 2008. Bacterial nonhomologous end joining ligases preferentially seal breaks with a 3′-OH monoribonucleotide. J. Biol. Chem. **283:**8331–8339. http://dx.doi.org/10.1074/jbc.M705476200.
21. **Timm J, Lim EM, Gicquel B.** 1994. Escherichia coli-mycobacteria shuttle vectors for operon and gene fusions to lacZ: the pJEM series. J. Bacteriol. **176:**6749–6753.
22. **Pitcher RS, Brissett NC, Picher AJ, Andrade P, Juarez R, Thompson D, Fox GC, Blanco L, Doherty AJ.** 2007. Structure and function of a mycobacterial NHEJ DNA repair polymerase. J. Mol. Biol. **366:**391–405. http://dx.doi.org/10.1016/j.jmb.2006.10.046.
23. **Nair PA, Smith P, Shuman S.** 2010. Structure of bacterial LigD 3′-phosphoesterase unveils a DNA repair superfamily. Proc. Natl. Acad. Sci. U. S. A. **107:**12822–12827. http://dx.doi.org/10.1073/pnas.1005830107.
24. **Zhu H, Wang LK, Shuman S.** 2005. Essential constituents of the 3′-phosphoesterase domain of bacterial DNA ligase D, a nonhomologous end-joining enzyme. J. Biol. Chem. **280:**33707–33715. http://dx.doi.org/10.1074/jbc.M506838200.
25. **Pitcher RS, Tonkin LM, Green AJ, Doherty AJ.** 2005. Domain structure of a NHEJ DNA repair ligase from Mycobacterium tuberculosis. J. Mol. Biol. **351:**531–544. http://dx.doi.org/10.1016/j.jmb.2005.06.038.
26. **Brissett NC, Pitcher RS, Juarez R, Picher AJ, Green AJ, Dafforn TR, Fox GC, Blanco L, Doherty AJ.** 2007. Structure of a NHEJ polymerase-mediated DNA synaptic complex. Science **318:**456–459. http://dx.doi.org/10.1126/science.1145112.
27. **Zhu H, Shuman S.** 2007. Characterization of Agrobacterium tumefaciens DNA ligases C and D. Nucleic Acids Res. **35:**3631–3645. http://dx.doi.org/10.1093/nar/gkm145.
28. **Henner WD, Grunberg SM, Haseltine WA.** 1982. Sites and structure of gamma radiation-induced DNA strand breaks. J. Biol. Chem. **257:**11750–11754.
29. **Nick McElhinny SA, Watts BE, Kumar D, Watt DL, Lundstrom EB, Burgers PM, Johansson E, Chabes A, Kunkel TA.** 2010. Abundant ribonucleotide incorporation into DNA by yeast replicative polymerases. Proc. Natl. Acad. Sci. U. S. A. **107:**4949–4954. http://dx.doi.org/10.1073/pnas.0914857107.
30. **Sparks JL, Chon H, Cerritelli SM, Kunkel TA, Johansson E, Crouch RJ, Burgers PM.** 2012. RNase H2-initiated ribonucleotide excision repair. Mol. Cell **47:**980–986. http://dx.doi.org/10.1016/j.molcel.2012.06.035.
31. **Hiller B, Achleitner M, Glage S, Naumann R, Behrendt R, Roers A.** 2012. Mammalian RNase H2 removes ribonucleotides from DNA to maintain genome integrity. J. Exp. Med. **209:**1419–1426. http://dx.doi.org/10.1084/jem.20120876.
32. **Teo SH, Jackson SP.** 1997. Identification of Saccharomyces cerevisiae DNA ligase IV: involvement in DNA double-strand break repair. EMBO J. **16:**4788–4795. http://dx.doi.org/10.1093/emboj/16.15.4788.
33. **Wilson TE, Grawunder U, Lieber MR.** 1997. Yeast DNA ligase IV mediates non-homologous DNA end joining. Nature **388:**495–498. http://dx.doi.org/10.1038/41365.
34. **Grawunder U, Zimmer D, Fugmann S, Schwarz K, Lieber MR.** 1998. DNA ligase IV is essential for V(D)J. recombination and DNA double-strand break repair in human precursor lymphocytes. Mol. Cell **2:**477–484. http://dx.doi.org/10.1016/S1097-2765(00)80147-1.
35. **Yan CT, Boboila C, Souza EK, Franco S, Hickernell TR, Murphy M, Gumaste S, Geyer M, Zarrin AA, Manis JP, Rajewsky K, Alt FW.** 2007. IgH class switching and translocations use a robust non-classical end-joining pathway. Nature **449:**478–482. http://dx.doi.org/10.1038/nature06020.
36. **Soulas-Sprauel P, Le Guyader G, Rivera-Munoz P, Abramowski V, Olivier-Martin C, Goujet-Zalc C, Charneau P, de Villartay J-P.** 2007. Role for DNA repair factor XRCC4 in immunoglobulin class switch recombination. J. Exp. Med. **204:**1717–1727. http://dx.doi.org/10.1084/jem.20070255.
37. **Han L, Yu K.** 2008. Altered kinetics of nonhomologous end joining and class switch recombination in ligase IV-deficient B cells. J. Exp. Med. **205:** 2745–2753. http://dx.doi.org/10.1084/jem.20081623.
38. **Chiruvella KK, Liang Z, Birkeland SR, Basrur V, Wilson TE.** 2013. Saccharomyces cerevisiae DNA ligase IV supports imprecise end joining independently of its catalytic activity. PLoS Genet. **9:**e1003599. http://dx.doi.org/10.1371/journal.pgen.1003599.
39. **Simsek D, Brunet E, Wong SY-W, Katyal S, Gao Y, McKinnon PJ, Lou J, Zhang L, Li J, Rebar EJ, Gregory PD, Holmes MC, Jasin M.** 2011. DNA ligase III promotes alternative nonhomologous end-joining during chromosomal translocation formation. PLoS Genet. **7:**e1002080. http://dx.doi.org/10.1371/journal.pgen.1002080.
40. **Paul K, Wang M, Mladenov E, Bencsik-Theilen A, Bednar T, Wu W, Arakawa H, Iliakis G.** 2013. DNA ligases I and III cooperate in alternative non-homologous end-joining in vertebrates. PLoS One **8:**e59505. http://dx.doi.org/10.1371/journal.pone.0059505.
41. **Boboila C, Oksenych V, Gostissa M, Wang JH, Zha S, Zhang Y, Chai H, Lee C-S, Jankovic M, Saez L-MA, Nussenzweig MC, McKinnon PJ, Alt FW, Schwer B.** 2012. Robust chromosomal DNA repair via alternative end-joining in the absence of X-ray repair cross-complementing protein 1 (XRCC1). Proc. Natl. Acad. Sci. U. S. A. **109:**2473–2478. http://dx.doi.org/10.1073/pnas.1121470109.
42. **Pannunzio NR, Li S, Watanabe G, Lieber MR.** 2014. Non-homologous end joining often uses microhomology: implications for alternative end joining. DNA Repair (Amst.) **17:**74–80. http://dx.doi.org/10.1016/j.dnarep.2014.02.006.